Material Characterizing through X-ray Diffraction

João P. S. Rodrigues
up201405201@fc.up.pt

May 24, 2018

Abstract

We demonstrate the X-ray diffraction technique in the study of both powder and sheet samples.

Two different crystal structures were studied using the technique, NaCl and W, the last one having been studied in both a powder and a sheet form. We determined the lattice constant of each sample ($a_{NaCl} = 5.65$ Å, $a_{Wpowder} = 3.1654$ Å, $a_{Wsheet} = 3.1677$ Å) with an error of less than 1%. The crystal structure of all samples was well characterized with the NaCl showing reflections from the planes expected for the simple cubic structure and the tungsten ones showing reflections for the BCC structure.

We report a preferential alignment of the NaCl sample to the 200 plane. The tungsten sheet sample also shows preferential alignment to the 200 plane while the powder sample exhibits a greater alignment to the 110 peak.

For each peak represented in the refraction plot of the samples, we found that there should be secondary, less intense peaks corresponding to the $K_{\alpha 2}$ and K_β lines of the Cu target.

Finally, the samples are analysed in terms of reflectivity. The sheet sample shows the greatest value for this parameter, since it is better aligned to the specific reflection planes of tungsten than the powder samples.

1 Introduction

The principle of X-ray characterization is Bragg diffraction of high energy photons on the atoms in the material that is being tested. This allows us to determine the direction of the crystal lattice planes in the material, thus determining which material it is.

In this experiment, two powders, NaCl and W, were characterized by X-ray diffraction, while for the second one, tungsten, a sheet sample was also tested in order to compare both of the structures.

The instrument used was the Rigaku Smartlab with a θ-θ geometry, Cu target and the Bragg-Brentano method. These choices will be explained further in the following subsections.

1.1 Bragg Diffraction

When radiation with a wavelength in the order of the atomic distances is scattered on a crystal, Bragg diffraction occurs. In such a material, the waves are scattered by the lattice planes, separated by a distance d. When the incident angle θ reaches a certain value (see Fig. 1), the waves interfere constructively, originating a much higher reflection power than for all the other angles. In order to achieve constructive interference, the waves must be in phase and thus, since the path difference between the two waves is $2dsin(\theta)$, we can define the Bragg condition as:

$$2dsin(\theta) = n\lambda \tag{1}$$

where λ is the wavelength of the incident light and n is the order of the diffraction.

By scanning the surface of the crystal with different values of θ and measuring the amount of reflected power, we can identify the directions of the lattice planes present in the crystal by relating the measured d with the Miller indices of the different planes. For example, for a cubic structure:

$$d_{hkl}^2 = \frac{a^2}{h^2 + k^2 + l^2} \tag{2}$$

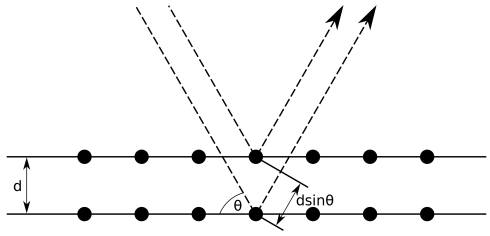

Figure 1: Bragg diffraction from a crystal lattice.

where a is the crystal lattice constant. Since a and the geometric structure are dependent on the material, we can accurately determine the material under inspection by using this technique.

1.2 X-ray Generation

This technique is dependent on the diffraction light's wavelength being of the order of the atomic distances. To achieve this, X-rays can be used since the common wavelengths of this type of light are on the order of the ångström (Å).

X-rays can be generated by a vacuum tube that uses a high voltage to accelerate the electrons, released by a filament, towards a target at a high velocity. The collision of the source electrons with the target excites an electron. When the electron transitions back to the fundamental state, an X-ray photon is released with a wavelength dependent on the target and the level from which the transition occurred, corresponding to a line on the X-ray spectrum (see Fig. 2) which can be either $K_{\alpha 1}$, $K_{\alpha 2}$ or K_{β}.

Depending on the application, the target should be chosen to provide the wavelength needed since a smaller wavelength can provide greater detail.

Finally, there are two types of generation methods available: stationary and rotating anode. The main difference between these two methods is the anode (target) movement on the rotating method which provides much better heat dispersion than the stationary technique. Thus, a choice must be made regarding the type of scans that will be performed with the equipment. If a higher dose or long scan times are required, a rotating anode should be used. If, otherwise, only short and relatively low intensity scans are to be made, then a stationary anode should suffice.

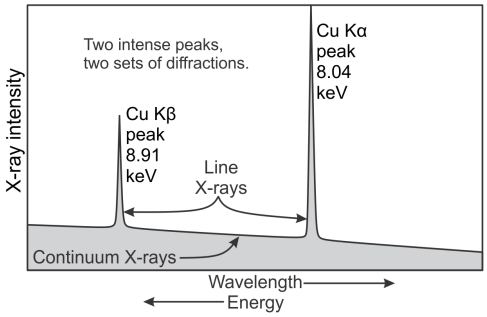

Figure 2: Cu target X-ray generation spectrum.

1.3 Instrument Choice

Before performing any X-ray measures, one must select the equipment which is going to be used. Some important factors to consider are:

- Source and detector geometry (θ-2θ vs θ-θ);
- X-ray source (stationary vs rotating anode);
- Target material (Cu, Mo, W, etc.);
- Beam geometry (focusing vs parallel beam).

The experiment geometry is highly dependent on the moving parts of the instrument. In Bragg diffraction, the incident beam is reflected by an angle of 2θ (θ being the incident angle) thus, when moving the sample by an angle of θ, the detector must move by an angle of 2θ in order to capture the reflected beam. This gives rise to the so-called θ-2θ geometry.

On the other hand, if one wishes to not move the sample, the instrument can move both the X-ray source and the detector. The geometry then becomes θ-θ since for a movement of θ on the source, the detector must move the same amount. This is the preferred geometry when working with powders - since we want to keep the sample unstirred to avoid the powder slipping from the crucible - and thus will be used in this experiment.

Another important choice is the X-ray generation method. This can be either stationary anode or rotating anode, as explained in Sec. 1.2. The Rigaku SmartLab uses a rotating anode configuration to deliver the maximum power and efficiency possible.

Furthermore, the target selection must be made beforehand since changing it is a highly technical and expensive task. In this experiment, a Cu target was

used and particularly, the K_α lines ($K_{\alpha1}$, $\lambda = 1.541\mathring{A}$ and $K_{\alpha2}$, $\lambda = 1.544\mathring{A}$) since a K_β filter - a fine Ni sheet that filters that specific wavelength - was used.

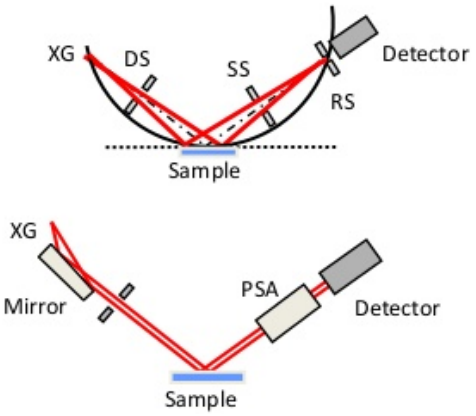

Figure 3: Bragg-Brentano (top) vs Parallel Beam (bottom) methods for X-ray diffraction.

Finally, there are two methods of diffracting the light on the sample: Bragg-Brentano and parallel beam (see Fig. 3). The main difference between the two is the angle between the interfering beams. Because the parallel beam method requires the use of a mirror and a PSA, the intensity of the method is lower than that of Bragg-Brentano and thus we should consider the amount of energy we need to use in our experiment, while choosing the configuration. On the other hand, the parallel beam configuration enables the study of the surface roughness of the sample which is of small interest when dealing with powders. Because of this, the Bragg-Brentano configuration was used in this experiment, even though the instrument allowed for a relatively simple change in geometry.

1.4 Procedure

The experimental procedure has some important steps:

1. Turning on the generator;
2. Preparing the sample;
3. Selecting the measurement package;
4. Aligning the optics;
5. Placing the sample on the platform;
6. Aligning the sample;
7. Running the measurement;
8. Turning the generator off or to idle.

The SmartLab Guidance software guides the user through the procedure [1].

Firstly, the generator should be turned on to full power in order to obtain the highest resolution possible. In the case of the Rigaku Smartlab, this is 45 kV and 200 mA. The standard safety procedure should be checked while performing this step.

The physical optical components should be placed in the instrument at this step. The slits used are of 5° for both the entrance and exit beam. A 10 mm ISL was also used. In the software, RS1 and RS2 were selected with 12 and 20 mm, respectively. A K_β filter should also be used on the exit path to allow for only the specific wavelengths of the K_α lines to be used in the experiment. The full list of parameters is available in Tab. 1.

In selecting the measurement package, one should choose the method of the scan - Bragg-Brentano or Parallel beam - and the resolution of the scan. After selecting the package, a flowchart guides the rest of the procedure: aligning the optics and the sample and running the measurement.

The optics alignment must be performed whenever the geometry is changed from Bragg-Brentano to Parallel beam or vice-versa, but can otherwise be skipped if no changes were made.

The sample should be prepared, at this step. To do so, both the NaCl and the W powder sample were grinded to a finer dust to promote a greater sample of planar orientation for the X-ray to detect. If the sample is a powder, it should be uniformly placed on the holder and pressed down in order to form a flat surface. When pressing down the sample, no transversal movement should be made so as to not favour any alignment of the sample's planes.

The main difference between both of the samples is the choice of sample holder - an aluminum one for the NaCl and a silicon one for the tungsten samples. The first one is a cheaper crucible and should be used when background influence is not important in obtaining the X-ray measurements, while the last one should be used for more sensitive measurements where we don't desire any reflections from the crucible - the silicon crystal can be cut with it's plane perpendicular to

	Slits			
	Soller (°)	ISL (mm)	PSA	Soller (°)
$NaCl_{powder}$	5	10	No	5
W_{powder}	5	10	No	5
W_{sheet}	5	10	No	5

	Sweep			
	Start (°)	Stop (°)	Step (°)	Speed (°/min)
$NaCl_{powder}$	15	90	0.01	8
W_{powder}	30	80	0.01	8
W_{sheet}	30	80	0.01	12

	Slits		
	IS (°)	RS1 (mm)	RS2 (mm)
$NaCl_{powder}$	0.5	12	20
W_{powder}	0.5	12	20
W_{sheet}	0.5	12	20

Table 1: Setup parameters for each of the samples studied.

the base of the crucible, thus not reflecting any X-ray light.

The sample holder should then be placed on the measuring platform with great care to not disturb the sample - since the platform is magnetic and could cause jitter when attracting the crucible.

The next step is to align the sample. This procedure scans the sample in a vertical movement in order to find its surface. This scan was made from -5 mm to -2 mm and the K_β filter should be previously removed to allow for the maximum amount of energy to reach the sensor. At this point, the experiment can be performed, as long as the K_β filter is reintroduced.

Finally, the generator should be turned off after the last experiment of the day is finished. Otherwise, it should be put on standby, using 20 kV and 10 mA.

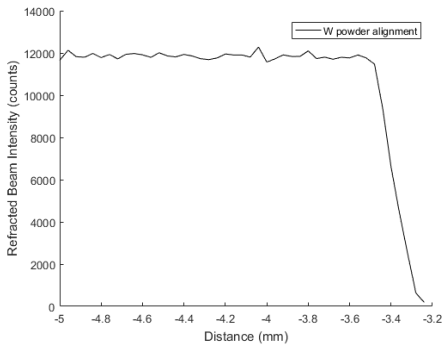

Figure 4: Alignment of the sample on the Z axis.

2 Results and Discussion

The experiment was performed on three samples: sodium cloride (NaCl) powder , tungsten (W) powder and a tungsten sheet.

As explained in Sec. 1.4, the first step towards doing any measurement is to align the sample holder in order to calibrate the zero point on the Z axis of the machine. An example plot of this alignment procedure is shown in Fig. 4. The process consists of displacing the X-ray source along the Z axis and measuring the refracted beam intensity. The zero point on the Z axis is calibrated as the point where the beam intensity is half way through the drop, which is about -3.4 mm in this particular case.

2.1 Sodium Cloride

The first sample measured was the NaCl powder which was carefully placed on an aluminum crucible. In Fig. 5, we can see the typical X-ray diffraction pattern for NaCl. For smaller 2θ values, we can see an almost linear decrease of the refracted beam intensity of the background which originates from diffraction from the air above the sample. The peaks of the graph were analysed in terms of θ position since each

Peak #	2θ (°)	θ (°)	d (Å)	$1/d^2$	n	hkl
1	27.35	13.68	3.27	0.09	3.00	111
2	31.69	15.85	2.83	0.13	4.00	200
3	45.42	22.71	1.99	0.25	8.00	220
4	56.44	28.22	1.63	0.38	12.00	222
5	66.20	33.10	1.41	0.50	16.00	400
6	75.27	37.64	1.26	0.63	20.00	420
7	83.96	41.98	1.15	0.75	24.00	422

Table 2: NaCl sample diffraction peak analysis.

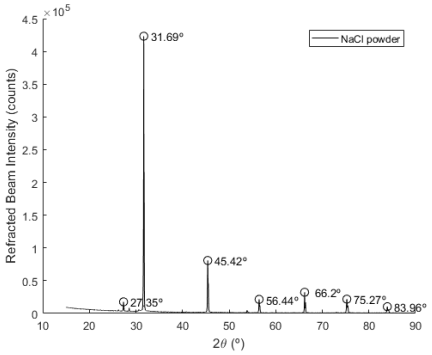

Figure 5: NaCl diffraction pattern.

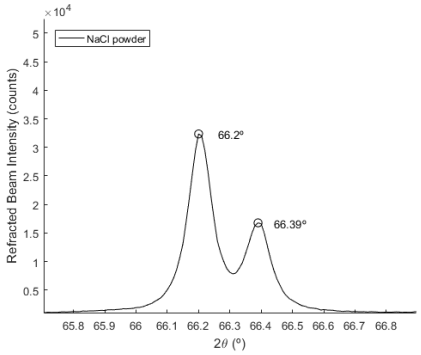

Figure 6: NaCl diffraction pattern zoom on the $66°$ peak.

of the peaks corresponds to a specific reflection from a lattice plane. These values can be processed in order to compute the planes present in the sample and determine it's structure.

The first step towards doing so is to calculate the interplane distance, d, corresponding to each a peak in the diffraction plot. The angle shown in the plot is in terms of 2θ and should thus be divided by 2 before applying Eq. 1. The considered peaks correspond to the $K_{\alpha 1}$ Cu line at $\lambda = 1.541$ Å.

We can then see, from Eq. 2, that,

$$\frac{1}{d_{hkl}^2} = nZ \tag{3}$$

where $n = h^2 + k^2 + l^2$ and $Z = 1/a^2$ where a is the lattice parameter. Thus, by finding the factor Z for which $1/(Zd^2)$ is an integer for all the values of d found from the reflection peaks, we can find the values of n and thus the miller indices of the peak refractions present in the sample. The value of Z for this particular sample is $Z = 0.0314$ $\mathring{A}^2$.

This data, organized in Tab. 2, shows us that the sample exhibits the expected simple cubic lattice reflections (any h, k, l).

We can also see that $a = 1/\sqrt{Z} = 5.65$ Å which represents a mere 0.2% deviation from the tabled $a_{NaCl} = 5.64$ Å so we can confirm that the sample is mainly NaCl.

Further analysis can be performed on Fig. 5 to determine what wavelengths of radiation are present in the refraction beam. By zooming in on the $66°$ peak, we can see (Fig. 6) that it is actually composed of a main and a secondary peak, each corresponding to a different wavelength on the source output. In the analysis above, we considered the main peak at $66.2°$, corresponding to the 400 plane. However, if we use the $K_{\alpha 2}$ wavelength to compute d for the $66.39°$, we see that this peak also corresponds to the same plane and thus originates from the $K_{\alpha 2}$ line. This secondary peak, also appears where we would expect from Eq. 1 since a higher wavelength should result in a higher value of θ.

Moreover, by inspecting the region of $2\theta = [27°, 32°]$, we can see the $27.35°$ peak corresponding to the 111 plane, to the left, and the $31.69°$ peak

Peak #	2θ (°)	θ (°)	d (Å)	$1/d^2$	n	hkl
1	40.27	20.13	2.24	0.20	2.00	110
2	58.26	29.13	1.58	0.40	4.00	200
3	73.21	36.61	1.29	0.60	6.00	211
1	40.24	20.12	2.24	0.20	2.00	110
2	58.22	29.11	1.58	0.40	4.00	200
3	73.18	36.59	1.29	0.60	6.00	211

Table 3: W samples diffraction peak analysis. Top: W powder; Bottom: W sheet.

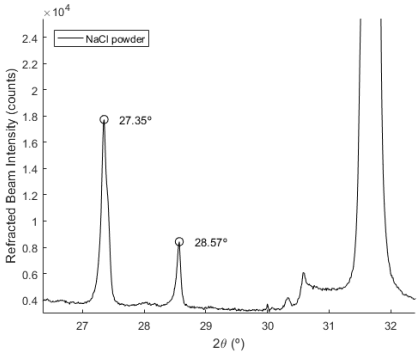

Figure 7: NaCl diffraction pattern zoom on the 27° - 32° region.

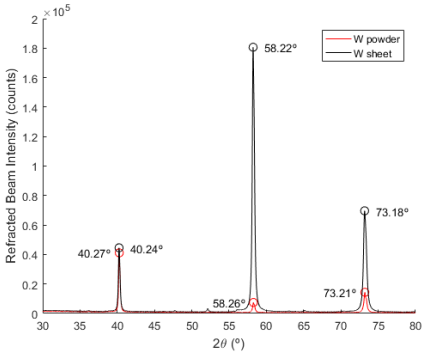

Figure 8: Bragg-Brentano vs Parallel Beam methods for X-ray diffraction.

corresponding to the 200 plane. However, between them we can see a well defined peak at $28.57°$ which should not correspond to any plane using the $K_{\alpha 1}$ and $K_{\alpha 2}$ lines. There remains only one possibility: the K_β filter is not 100% efficient in filtering this $\lambda = 1.392$ Å Cu line and thus, this peak would appear because of the reflection from the 200 plane. This can be confirmed by calculating the expected angle for this reflection at that wavelength,

$$2\theta = 2 * \arcsin\left(\frac{\lambda}{2d}\right) = 28.56° \qquad (4)$$

which is only $0.01°$ from the obtained value of the peak.

This analysis seems to indicate that all the peaks present in Fig. 5 should be accompanied by secondary $K_{\alpha 2}$ and K_β peaks which should not be confused for further planar reflections.

2.2 Tungsten

By performing the same analysis for the tungsten samples, we arrived at Fig. 8, overlaying the refraction patterns of both samples. A first inspection of this plot reveals the expected outcome from analysing samples from the same material: the main peaks coincide closely since they represent reflections from the same plane. In fact, the greatest difference between the angular value of two peaks is just $0.04°$.

Furthermore, we can almost immediately discern the enormous difference in scale for the central peak for the two different types of samples. For the W sheet, this peak, at $59.22°$, is the highest of the three while, for the powder sample, this reflection, at $58.26°$, yields the smallest intensity from the three reflections observed. This can be readily explained by considering that the powder sample's reflection planes should be randomly aligned and thus reflect more uniformly across all the possible reflections. On the other hand, the sheet sample is aligned to a specific plane which, in this case, exhibits a reflection at $58.22°$ corresponding to the 200 plane (Tab. 3).

a_{powder} (Å)	a_{sheet} (Å)	a_{tabled} (Å)
3.1654	3.1677	3.1652

Table 4: Lattice parameter for W obtained from the powder and sheet samples and tabled value.

$NaCl_{powder}$	W_{powder}	W_{sheet}
3.4e3	1.2e3	4.0e3

Table 5: Sum of intensity values in number of counts divided by number of angles measured, for all the samples.

We can further analyse this samples by calculating the miller indexes of each peak reflection. The results are shown in Tab. 3. Using the determined value of $Z_{powder} = 0.0998$ and $Z_{sheet} = 0.0997$, we can compute the lattice parameter for each of the samples (Tab. 4). We can thus confirm that the samples are mainly tungsten with an error of less than 1%. Besides that, the sample also shows the typical reflections for a BCC lattice ($h + k + l = even$), which is the case of tungsten.

Finally, we can do a brief analysis on the samples' reflection amount. By summing the intensity values for all the samples, we can determine the net amount of light that reached the detector, after diffracting on the samples. The result of this calculation (Tab. 5) shows that the tungsten sheet sample is the most reflective, having $4.0e3$ counts per angle. The NaCl sample comes in second place with $1.4e3$ less reflections per measurement taken. The less reflective sample is the W_{powder}. This lack of reflectivity could be explained by the uniformity of each of the powder's crystal's alignment which results in smaller peaks at the angles where reflection takes place. On the other hand, the NaCl sample, even though it is also a powder, presents reflections from more planes than the W one which contributes to increasing the number of total counts.

3 Conclusions

The present work's aim was to demonstrate the X-ray diffraction technique in the study of both powder and sheet samples.

Two different crystal structures were studied using the technique, simple cubic (NaCl) and body centered cubic (BCC, W), the last one having been studied in both a powder and a sheet form. Both samples were confirmed to be mainly composed of their respective material with an error of less than 1% for the determined lattice constant ($a_{NaCl} = 5.65$ Å, $a_{Wpowder} = 3.1654$ Å, $a_{Wsheet} = 3.1677$ Å). Moreover, the crystal structure of all samples was well characterized since the NaCl one showed the classical simple cubic refraction planes (ex. 111, 200, 220, etc.) while the tungsten ones showed the BCC structure (ex. 110, 200 and 211). We also found that the NaCl sample is preferentially aligned to the $2\theta = 31.69°$ reflection corresponding to the 200 plane. The tungsten sheet sample also shows preferential alignment to the 200 plane while the powder samples has a greater reflection at the 110 peak.

This work also shows that, for each peak represented in the refraction plot of the samples, there should be secondary, less intense peaks for the wavelengths of the $K_{\alpha 2}$ and K_{β} lines of the Cu target.

Finally, the samples were analysed in terms of reflectivity by computing the number of counts per measured angle. The sheet sample shows the greatest value for this parameter, since it is better aligned to the specific reflection planes of tungsten than the powder samples.

References

[1] *Basic XRPD and Thin Film Analysis on the Rigaku Smartlab Diffractometer*.